IDENTIFYING MINERAL CANDIDATES IN HIGH-RESOLUTION GEOCHEMICAL DATA WITH APPLICATION TO PIXL ON MARS 2020. K. L. Siebach[1] G. Costin[1], and Y. Jiang[1], [1]Department of Earth, Environmental, and Planetary Science, Rice University, Houston, TX 77005 (contact: ksiebach@rice.edu).

Introduction: Compositional data from the surface of Mars have been used for decades to describe the character of Martian surfaces at planetary scales (e.g., Gamma-Ray Spectrometer data [1]) and at rover scales (e.g., Pathfinder, MER, and MSL APXS data, MSL ChemCam data [2-4]). Geochemical data provide critical constraints on the bulk composition of the surface of the planet or specific rocks, but they must be interpreted to constrain geological processes and habitability. For example, an increase in MgO has very different implications if the MgO is contained in olivine, where it may be a signature of the igneous protolith and an indication of minimal water-rock interaction, vs in magnesium sulfate, which is produced in the final stages of evaporation or freezing. Interpretations of the co-varying elements in compositional maps have frequently been used to infer minerals and their abundances [5-8], or the elemental maps have been correlated with results from instruments designed to measure mineralogy to infer chemistry of amorphous phases [9, 10]. Here, we describe our approach to an algorithm that will be used to automatically identify putative minerals in high-resolution geochemical data, with application to the Planetary Instrument for X-ray Lithochemistry (PIXL) [11] on the Perseverance rover.

PIXL Instrument: PIXL is a micro-focus X-ray fluorescence spectrometer mounted to the robotic arm of the Perseverance rover. The compositional data returned from PIXL instrument, correlated with high-resolution color imagery from WATSON, will provide the highest resolution maps of elemental abundances ever produced for *in-situ* Mars samples, with PIXL spot sizes as fine as 125 µm (i.e., fine sand size grains and above [12]). This dataset will provide a new opportunity to investigate the chemistry of rocks at a scale approaching the grain sizes of individual minerals and detrital grains, allowing much finer-scale derivation of likely mineral components.

Classification groups: We identify a list of observed, or likely, minerals on Mars based on the list provided by Salvatore et al. [13] and augmented by MSL and CRISM analyses. Sixty-one mineral phases are considered, which we sorted into 19 groups: (1) Sulphate, (2) Phosphate, (3) Halide, (4) Amphibole and Pyroxene, (5) Carbonate, (6) Chlorite, (7) Fe-oxides and hydroxides, (8) Fe-Ti-oxide (ilmenite), (9) Feldspar, (10) Kaolinite, (11) Mica, (12) Olivine, (13) Saponite, (14) Serpentine, (15) SiO_2-glass, (16) SiO_2 polymorph, (17) Smectite, (18) Talc, and (19) Zeolite. Some of these groups are represented by one single mineral species (e.g., Fe-Ti-oxide is ilmenite, only, whereas a Ti-Magnetite, due to its high variability in TiO_2, is considered part of the Fe-oxide group). Other groups contain multiple minerals, e.g., sulphates include Ca, Mg, and Fe sulphates.

Stoichiometric mineral identification: Stoichiometric and elemental constraints from PIXL are able to distinguish most of the minerals observed by Mars Science Laboratory and those observed by CRISM and TES orbital instruments over the Jezero crater site [13, 14]. Similar, although manual, techniques have been used to identify the mineral compositions of minerals observed by ChemCam on MSL *Curiosity* [15, 16], and such techniques are commonly used on Earth to identify minerals from Electron Micro-Probe Analyzer (EPMA) datasets [17-19]. There are limitations when deriving mineralogy from compositional data, for example mineral polymorphs cannot be distinguished, but the rapid identification of potential minerals is still valuable.

We tested our initial algorithm on 2,009 compositional observations from EPMA analyses of minerals and derived mineral chemistries. The test set contained chemical analyses representing selected natural and ideal compositions for minerals belonging to all 19 mineral groups. The code correctly categorized 1,973 analyses into the 19 groups, and correctly did not categorize 13 Cr-spinel analyses that were included to check for false positives. The remaining 23 analyses were found to be mislabeled in our test set, so they were also accurately categorized as not in the 19 groups.

Algorithm: A first-order criterion in our algorithm separates mineral oxides and salts, including iron oxides, Fe-Ti oxides, carbonates, silica, sulfates, phosphates, and halides that are characterized by specific elements present in high concentration and/or by missing other elements (Fig. 1). For example, sulfates are characterized by high SO_3 values and low values of other anionic molecules.

To categorize minerals in silicate groups, we begin by recognizing that each mineral group is characterized by an ideal formula. Within each group, certain cations occupy specific crystallographic positions in the mineral lattice, coordinated by a specific number of oxygen atoms. These crystallographic positions are reflected in the element's position in the formula of a mineral. Some elements have high geochemical

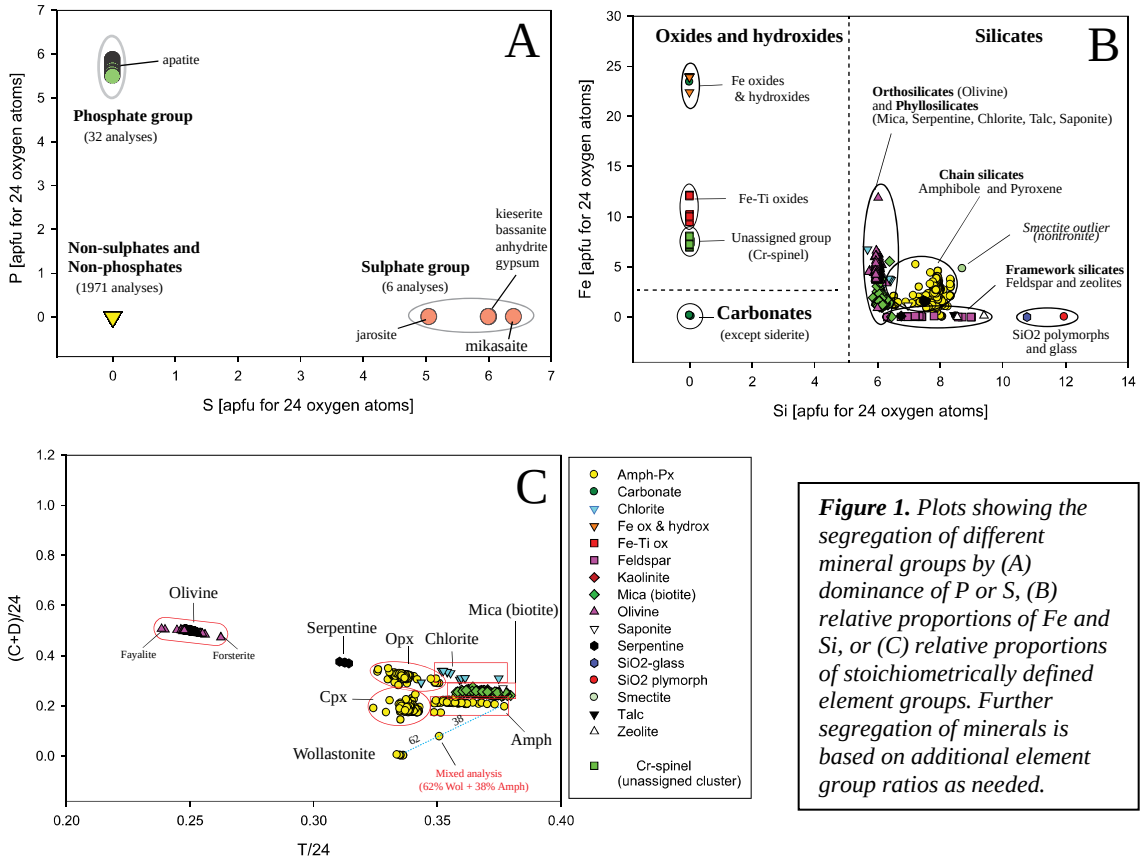

Figure 1. *Plots showing the segregation of different mineral groups by (A) dominance of P or S, (B) relative proportions of Fe and Si, or (C) relative proportions of stoichiometrically defined element groups. Further segregation of minerals is based on additional element group ratios as needed.*

affinities and can replace each other, and, therefore, most mineral species may have specific possible elemental substitutions. These substitutions do not affect the ideal formula of the mineral group. From this understanding, we derived a general formula for all considered minerals represented by $A_mB_nC_oD_pT_rO_{24}$, where A, B, C, D, are cations in non-tetrahedral coordination, T are cations in tetrahedral coordination, and m, n, o, p, r are stoichiometric coefficients.

A = Na + K
B = Ca + Mn + Sr
C = Mg + Fe* + Mn + Ni + Zn
D = Al (VI)* + Cr + Ti + Fe^{3+}
T = Si + Al (IV) + S + P

To divide silicate mineral groups, we use different ratios of cations (all normalized to 24 equivalent oxygens), like the example shown in Figure 2C, to identify likely mineral groupings. With appropriate criteria, using stoichiometrically interchangeable element sets A, B, C, D, and T, all 19 mineral groups can be identified and distinguished. After silicate mineral grouping, the cations for each analysis in each group are re-normalized to the number of equivalent oxygen atoms characteristic of the ideal formula of the group (e.g., 4 oxygens for olivine, 6 oxygens for pyroxene, 23 oxygens for amphibole, etc). The tetrahedral and octahedral Al and Fe^{3+} estimation is done by stoichiometry, and the C, D, and T element groupings shown above are recalculated with stoichiometrically appropriate amounts of Al and Fe. The output of this stage will include a stoichiometric formula calculation for each analysis in each group, a calculation of mean and standard deviation for each cation, and a calculation of meaningful compositional indicators (Fo in olivine, An in plagioclase, En-Wo-Fs in pyroxene etc.).

References: [1] Saunders, R.S., et al. (2004) *SSR*. 110(1/2): p. 1-36. [2] Gellert, R., et al. (2006) *JGR*. 111(E2). [3] Rieder, R., et al. (1997) *Science*. 278: p. 1771. [4] Wiens, R.C., et al. (2012) *SSR*. 170(1-4): p. 167-227. [5] VanBommel, S.J., et al. (2016) *X-Ray Spectrometry*. 45(3): p. 155-161. [6] Siebach, K.L., et al. (2017) *JGR*. 122(2): p. 295-328. [7] Ruff, S.W. and J.D. Farmer (2016) *Nat. comm*. 7: p. 13554. [8] McLennan, S.M., et al. (2005) *EPSL*. 240(1): p. 95-121. [9] Dehouck, E., et al. (2014) *JGR*. 119(12): p. 2640-2657. [10] Smith, R.J., et al. (2018) *JGR*. 123. [11] Allwood, A.C., et al. (2020) *SSR*. 216(8). [12] Wentworth, C.K. (1922) *J. Geol*. 30(5): p. 377-392. [13] Salvatore, M.R., et al. (2018) *Icarus*. 301: p. 76-96. [14] Goudge, T.A., et al. (2015) *JGR*. 120(4): p. 775-808. [15] Cousin, A., et al. (2017) *Icarus*. 288: p. 265-283. [16] Payré, V., et al. (2020) *JGR*. 125(8). [17]McGee, J.J. and K. Keil (2001) *Microanal*. 7(2): p. 200-210. [18]Shimizu, M., et al. (2019) *Island Arc*. 28(2). [19]Zhao, D., Y. Zhang, and E.J. Essene (2015) *Ore Geology Reviews*. 65: p. 733-748.